Phase separation of monomer in liquid crystal mixtures and surface morphology in polymer-stabilized vertical alignment liquid crystal displays

# Phase separation of monomer in liquid crystal mixtures and surface morphology in polymer-stabilized vertical alignment liquid crystal displays

**Jae Jin Lyu**[1,2,4]**, Hirotsuku Kikuchi**[2]**, Dae Hyun Kim**[3]**, Jun Hyup Lee**[1]**, Kyeong Hyeon Kim**[1]**, Hiroki Higuchi**[2] **and Seung Hee Lee**[3,4]

[1] Development Center, LCD Business, SAMSUNG Electronics Co. LTD., Tangjeong-Myeon, Asan, Chungnam 336-741, Korea
[2] Institute for Materials Chemistry and Engineering, Kyushu University, 6-1 Kasuga-Koen, Kasuga 816-8580, Japan
[3] Department of BIN Fusion Technology and Department of Polymer-Nano Science and Technology, Chonbuk National University, Jeonju, Jeonbuk 561-756, Korea

E-mail: jsquare.lyu@samsung.com and lsh1@chonbuk.ac.kr

## Abstract

The polymer-stabilized vertically aligned (PS-VA) liquid crystal display (LCD) driving mode has high potential for manufacturing low power consuming displays due to the higher transmittance and fast response as compared with the existing patterned vertically aligned and multi-domain vertically aligned modes. In this paper we have investigated the reaction mechanisms of monomer–liquid crystal blends to form a surface pre-tilt angle of liquid crystal in vertical alignment LCD associated with a fishbone electrode structure. The observed sizes of polymer bumps formed on the substrates were found to be dependent on the exposed UV wavelength and were almost equal in both top and bottom substrates. When a large UV wavelength was used, the phase separation mechanism of monomer in PS-VA mode was found nearly isotropic rather than anisotropic in contrast to the previous studies.

(Some figures in this article are in colour only in the electronic version)

## 1. Introduction

The market of liquid crystal displays (LCDs) has grown rapidly in recent times due to the dual effects of performance enhancement and price reduction. From the performance viewpoint, fast response time, wide viewing angle and high contrast ratio are the key requirements for high-quality LCDs. The liquid crystal (LC) modes used for manufacturing display devices can be broadly divided into two distinct categories in accordance with the initial alignment of LC molecules and the direction of the applied electric field. One is the homogeneous alignment mode which uses in-plane and fringe electric fields to rotate the LC director almost in plane, called in-plane switching [1] and fringe-field switching [2–6], respectively. The other is rubbing-free vertical alignment (VA) [7–9] mode in which many different approaches are commercialized. In particular, VA mode has realized excellent dark state because the polarization state of the incident linearly polarized light is not changed while passing through the LC layers. Achieving a good dark state is very important in display applications and hence a number of display manufacturing companies employ VA mode for manufacturing large-sized displays. The VA mode can be divided into a few categories depending on the controlling schemes of LC domains such as patterned VA [10, 11] using the patterning of transparent electrodes, multi-domain VA [12, 13] using the protrusion. However, some drawbacks have been pointed out in these VA display

[4] Authors to whom any correspondence should be addressed.

modes such as transmittance loss due to improper control of
LC domains and slower response time due to random motion of
vertically aligned LC molecules [14]. Recently, photo-aligned
UV vertical alignment [15] (UV$^2$A) and polymer-stabilized
vertical alignment (PS-VA) [16–21] modes in which surface tilt
angle instead of perfect VA is defined over the whole surface are
introduced to improve the performance of VA mode displays.

In PS-VA mode, a small amount of ultra-violet (UV)
curable monomer is added to the LC mixture and then the
cell is exposed to UV radiation applying a voltage larger
than the threshold. Then phase separation of the monomer
from the LC mixture occurs during UV exposure. In fact,
before PS-VA mode, several LC modes such as polymer-
dispersed LC, polymer-stabilized nematic LC, phase-separated
composite organic film (PSCOF) [22, 23] and so on, which
exploited the advantage of UV curing for producing displays,
were proposed. In the case of PSCOF, phase separation
mechanism is explained by a photo-polymerization-induced
phase separation. The UV-curable monomers move to the
glass substrate nearest to the UV exposure in this case and are
polymerized on that surface, and this is called anisotropic phase
separation. However, our studies on the PS-VA mode have
confirmed that the surfaces of the top and bottom substrates
have nearly the same polymer bump density. Therefore,
the phase separation mechanism is totally different from the
anisotropic phase separation, as we have reported in this
paper. Here, we report the reaction mechanism of UV-curable
monomers according to the wavelength of UV and investigate
the surface morphology formed by the polymerized monomers
using scanning electron microscopy (SEM) measurements.

## 2. Experimental

The cell for the present investigation was prepared by
sandwiching a couple of transparent indium tin oxide (ITO)
coated glass substrates. The ITO coating was patterned in
a fishbone shape on the bottom substrate; however, the top
substrate was made of plain ITO-coated glass. A cell gap of
$3.5\,\mu$m was uniformly maintained using plastic ball spacers.
The top view of the micro-slit structure of PS-VA mode is
shown in figure 1. The polymer type of VA layer was coated
on both substrates with a thickness of $1000\,\text{Å}$. The fishbone
structure allowed the LC molecule to tilt symmetrically in all
quadrants over the electrode in the presence of a sufficient
field. The fishbone electrode conditions were as follows:
the width of the slit electrode ($w$) was $3\,\mu$m and the inter
electrode distance ($l$) was $4\,\mu$m. The present investigation
was carried out using the LC mixture obtained from Merck
(Korea), having a negative dielectric anisotropy ($\Delta\varepsilon$) of $-3.2$,
birefringence ($\Delta n$) of 0.1 and nematic to isotropic transition
temperature of $80\,^\circ$C. A commercial diacrylate monomer of
0.5 wt% called reactive mesogen (RM) was added to the host
LC mixture and filled into the previously discussed cell. The
polymerization process for device fabrication was investigated
under different UV wavelengths of 365, 334 and 313 nm, using
a high-pressure mercury UV lamp attached with various band
pass filters. The intensity of UV light was controlled from
30 to $100\,\text{mW}\,\text{cm}^{-2}$ by tuning the ac power attached with



**Figure 1.** Micro-slit structure of PS-VA mode.

this experimental set-up. The SEM imaging of the cells was
performed after removing the LC using n-hexane solvent. The
phase retardation values of the prepared devices were measured
using 69050-axo (Axometrics Co.) which led us to estimate
the surface pre-tilt angles under different UV conditions.

## 3. Results and discussion

In the PS-VA mode, the alignment surface induces surface
tilt angle uniformly on LC molecules by polymerization of
monomer in the LC mixture with UV curing and the formed
polymer grains on the surfaces are evenly distributed over the
whole LC layer. However, the mechanism of polymerization
process has never been clearly reported. The following
equation demonstrates the critical factors of a polymerization
reaction:

$$\frac{-\text{d}[M]}{\text{d}t} = R_\text{p} = k_\text{p}[M]\left(\frac{\phi\varepsilon I_0 b}{k_\text{t}}\right)^{1/2}[M]_0 e^{-k_\text{d}\cdot t/2} \quad (1.1)$$

where $[M]$ and $R_\text{p}$ are the total concentration of UV curable
monomer and the polymerization rate, $k_\text{p}$, $k_\text{d}$ and $k_\text{t}$ are the
propagation, initiation and termination rate constants, $[M]_0$
is the initial concentration of the UV-curable monomer, $\phi$
is the quantum yield of initiation, $I_0$ is the initial intensity
of light, $\varepsilon$ is the molar absorptive extinction coefficient and
$b$ is the cell thickness. This equation provides the way to
control the polymerization process by controlling the rate
of polymerization using easily tunable parameters, such as
monomer concentration, intensity of incident light and cell
gap. Hence the polymerization process can be optimized by
tuning these variables.

The monomer structure is composed of a pair of benzene
rings and additional functional groups at terminal positions as
shown in figure 2. The absorption spectra of the monomer
are determined in $0.0001\text{M}\,\text{l}^{-1}$ acetone solution using an
absorption spectrometer, and are depicted in figure 3. The
monomer absorbs UV radiation and hence the spectrum is

peaked at a wavelength less than 300 nm. As the photo-polymerization rate strongly depends on the energy of incident radiation, the polymerization process can be accelerated at wavelengths less than 300 nm and in the 365 nm range of wavelength the polymerization rate is relatively low. We have carefully controlled the curing wavelength of UV since strong radiation may damage the host LC materials and the alignment layer.

The fabrication process of the PS-VA device is depicted in figure 4. The LC–monomer blend is filled into the previously described cell structure. In the initial state, both LC and RM are vertically aligned by the VA layer on both substrates. When an operating voltage is applied to the cell, a tilt angle is generated over both top and bottom substrates above the
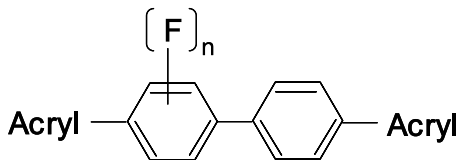


**Figure 2.** General structural formula of the monomer.
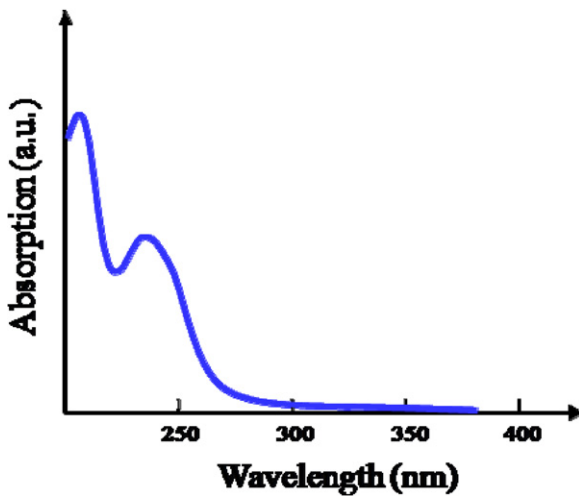


**Figure 3.** Absorption spectrum of the used commercial UV-curable monomer.

VA layer and fixed by the micro-slit pattern formed on the bottom fishbone-patterned substrate. At this state, the first UV exposure polymerizes a major part of the monomer in the LC blend on the surfaces of the VA layer for both substrates. At the next stage, the applied voltage is removed and then the cell is again exposed to UV for a second time to remove any residual monomer. Finally, the polymer chain is formed on the surfaces of both substrates without any residual monomer in the LC bulk layer.

Figure 5 shows the relation between the supplied energy in the first UV exposure and surface tilt angle. It is evident from figure 5 that the growth of pre-tilt angle is proportional to the energy supplied by the UV source.

In order to analyse the surface morphology formed by the polymerized monomer, the LC is removed from the devices prepared under different wavelengths of UV irradiation. The cells are disassembled to characterize the substrates using the SEM imaging technique, as shown in figure 6. The figures show polymer bumps of varying sizes. The sizes of the polymer bumps are found to be smaller for shorter wavelengths of irradiated UV. For UV irradiation wavelength of 313 nm (figure 6(*a*)) the polymer bumps appearing on the top substrate are quite different from those on the bottom one. This is due to higher UV absorption (figure 3) on the top substrate in comparison with the bottom one at this wavelength. As the reaction rate is increased with reduction in UV wavelength, the top substrate shows smaller polymer bumps than the bottom substrate. However, with increasing wavelength of UV, that is, on reducing the energy delivered to the cells, the size of the polymer bumps appearing on both substrates becomes comparable as observed in figure 6(*b*)—334 nm and 6(*c*)—365 nm. Thus, it is better to reduce the rate of polymerization for achieving homogeneity as well as an optimal size for the polymer bumps. Again, short wavelengths may damage the LC host and organic materials including the alignment layer. Accordingly, a wavelength of 365 nm is advisable for acquiring the same characteristics on both substrates without any damage. As a result of equal distribution of similar polymer bump size in both substrates, we can assume that the isotropic phase separation has occurred under a specific wavelength condition. Figure 7 depicts the vertical image of
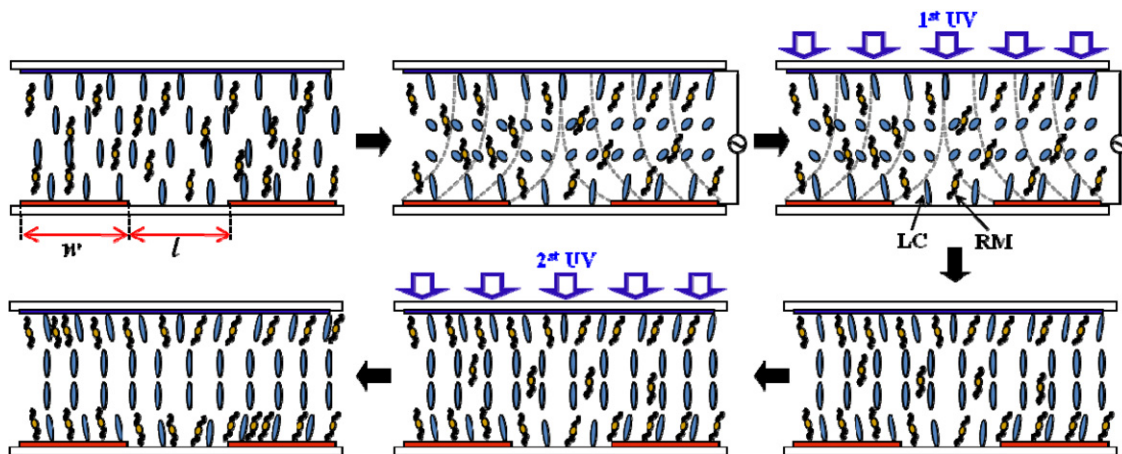


**Figure 4.** Schematic representation of PS-VA device fabrication.
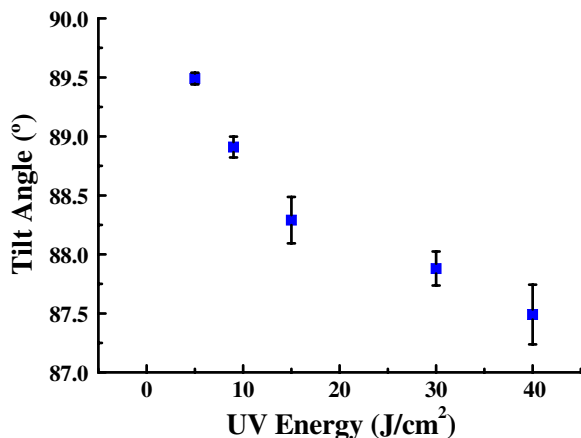
**Figure 5.** Pre-tilt over LC as a function of energy delivered by first UV exposure.



**Figure 7.** Vertical SEM image of 20 000 times magnified assembled cell having gap 3.5 $\mu$m. The dark image indicates no polymer network in the bulk of LC layer.
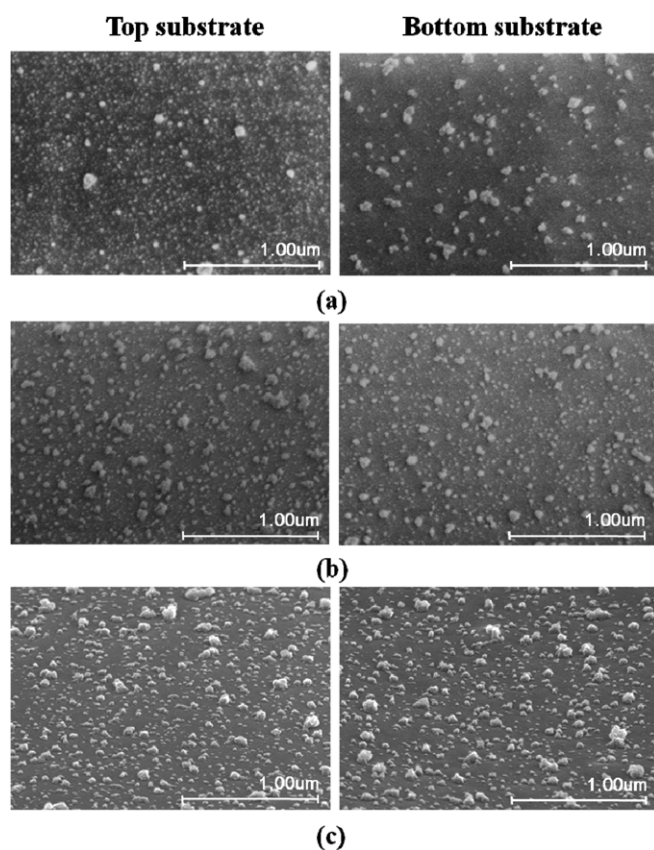


**Figure 6.** Comparison of polymer bumps of top and bottom substrates of the decoupled device by 50 000 times magnified SEM imaging.
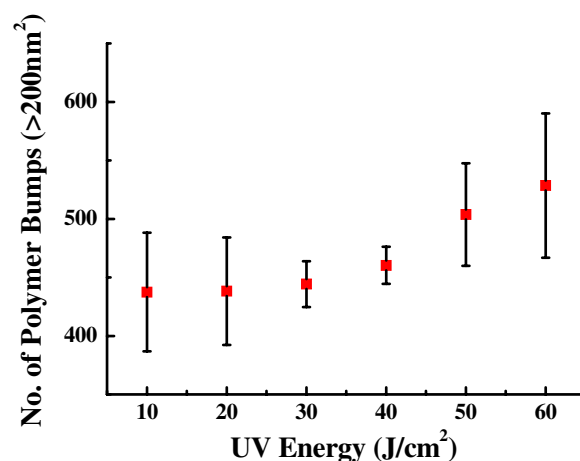


**Figure 8.** Number of polymer bumps as a function of energy delivered by first UV exposure.

the assembled cell after removing the liquid crystal. The figure proves the absence of polymer network in the middle layer of the cell as it appears dark in the image. This phenomenon is observed at a very low concentration of monomer and hence it can be expected that the content of monomer is so less to form the bulk polymer network in this case assuming that the monomer moves to the alignment surface or separates in phase before UV curing. From the SEM images, the number of polymer bumps appearing in a fixed area is counted using the image J 1.43u software (Wayne Rasband National Institutes

of Health, USA). Figure 8 shows the relationship between the density of polymer bumps and exposed UV energy. As shown in this figure, we can confirm that the number of polymer bumps is increased gradually at 20 J cm$^{-2}$. In particular, the density of polymer bumps is found to be similar in the top and bottom substrates.

Figure 9 shows the phase separation modelling of PS-VA mode. Based on SEM images, two possible phase separations of monomer along the LC layers, isotropic and anisotropic, can be considered. In the isotropic phase separation, the monomer's concentration is higher in the vicinity of the alignment surface and relatively lower in the middle layer possibly due to surface interaction energy difference between the LC-VA layer and the monomer-VA layer (see figure 9(*a*)), resulting in a phase separation between the monomer and the LC before UV exposure. In other words, the majority of the monomer content in the monomer-LC blend reacts at the alignment surface and a small amount of monomer participates in the middle layer by diffusion migration. Consequently, the polymer bumps are formed equally on the top and bottom substrates with similar sizes especially under exposure of long-wavelength UV. However, in the anisotropic phase separation, as in the case of PSCOF, the monomers are uniformly dispersed
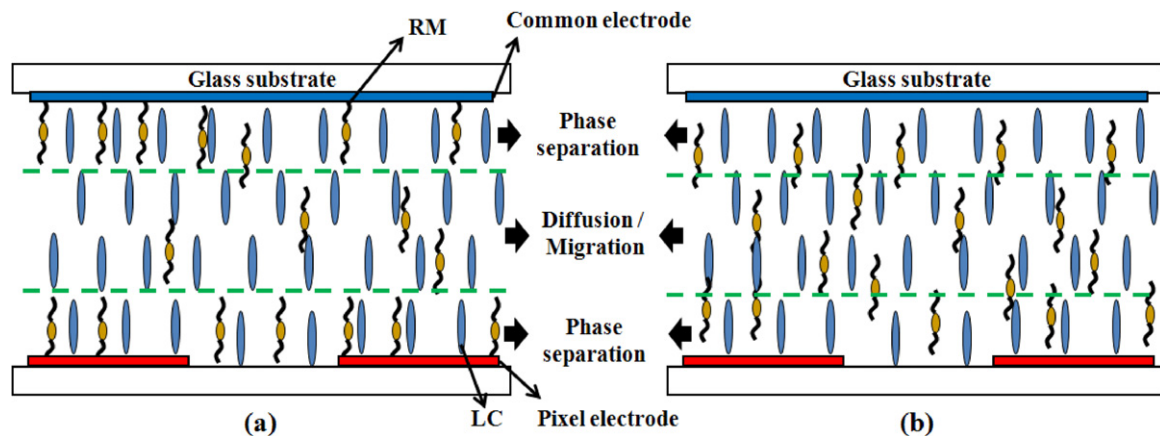
**Figure 9.** Schematic representation showing phase-separated monomer before first UV exposure in PS-VA cells: (*a*) proposed model and (*b*) conventional model.

so that the concentration of monomer is constant along the LC layer without any gradient phase separation between LC and monomer (see figure 9(*b*)). Then, the photo-induced reaction starts immediately from the side of the substrate where it is exposed to UV radiation, and eventually the monomer moves to the substrate surface, forming polymer bumps or networks only on the side of UV exposure.

In the case of PS-VA cell, the monomer reaction is estimated in the isotropic phase separation, which means the monomer moves to both substrates before UV exposure, and polymer bump is formed evenly on both surfaces. This paper also shows the importance of the UV curing process associated with the wavelength of the incident light in achieving isotropic phase separation in PS-VA mode.

## 4. Summary

We have studied the phase separation process of a monomer from a LC–monomer mixture in new-generation LCD technology PS-VA mode which provides high transmittance and fast response time. The displays in the said mode are prepared by two-step UV curing processes using a small amount of monomer (0.5 wt%) in LC. The typically optimized processing technique produces LC's surface tilt angle over the substrate by entangled polymer bumps and a longer UV wavelength than 313 nm generates equally distributed size and number of polymer bumps. We assume that the isotropic phase separation occurs before UV exposure, which is also supported by the SEM images on the alignment surface.

## Acknowledgment

## References

[1] Oh-e M and Kondo K 1995 *Appl. Phys. Lett.* **67** 3895
[2] Lee S H, Lee S L and Kim H Y 1998 *Appl. Phys. Lett.* **73** 2881
[3] Hong S H, Park I C, Kim H Y and Lee S H 2000 *Japan. J. Appl. Phys.* **39** L527
[4] Lee S H, Kim H Y, Lee S M, Hong S H, Kim J M, Koh J W, Lee J Y and Park H S 2002 *J. Soc. Inform. Disp.* **10/2** 117
[5] Yu I H, Song I S, Lee J Y and Lee S H 2006 *J. Phys. D: Appl. Phys.* **39** 2367
[6] Jung J H, Ha K S, Chae M, Srivastava A K, Lee H K, Lee S-E and Lee S H 2010 *J. Korean Phys. Soc.* **56** 548
[7] Ohmuro K, Kataoka S, Sasaki T and Koike Y 1997 *Soc. Inform. Disp. Tech. Dig.* **28** 845
[8] Wu S-T 1994 *J. Appl. Phys.* **76** 5975
[9] Lien A, Cai C, Nunes R W, John P A, Galligan E A, Colgan E and Wilson J S 1998 *Japan. J. Appl. Phys.* **37** 597
[10] Kim K H, Lee K H, Park S B, Song J K, Kim S N and Souk J H 1998 *Proc. 18th Int. Display Res. Conf. and Asia Display '98* (San Jose, CA: Society for Information Display) p 383
[11] Kim S S, Berkely B H, Kim K H and Song J K 2004 *J. Soc. Inform. Disp.* **12/4** 353
[12] Koma N, Baba Y and Matsuoka K 1995 *Soc. Inform. Disp. Tech. Dig.* **26** 869
[13] Takeda A, Kataoka S, Sasaki T, Chida H, Tsuda H, Ohmuro K, Sasabayashi T, Koike Y and Okamoto K 1998 *Soc. Inform. Disp. Tech. Dig.* **29** 1077
[14] Lee S H, Kim S M and Shin-Tson Wu 2009 *J. Soc. Inform. Disp.* **17** 551
[15] Miyachi K, Kobayashi K, Yamada Y and Mizushima S 2010 *Soc. Inform. Disp. Tech. Dig.* **41** 579
[16] Hanaoka K, Nakanishi Y, Inoue Y, Tanuma S, Koike Y and Okamoto K 2004 *Soc. Inform. Disp. Tech. Dig.* **35** 1200
[17] Kim S G, Kim S M, Kim Y S, Lee H K, Lee S H, Lee G-D, Lyu J-J and Kim K H 2007 *Appl. Phys. Lett.* **90** 261910
[18] Kim S M, Cho I Y, Kim W I, Jeong K-U, Lee S H, Lee G-D, Son J, Lyu J-J and Kim K H 2009 *Japan. J. Appl. Phys.* **48** 032405
[19] Kim S G, Kim S M, Kim Y S, Lee H K, Lee S H, Lyu J-J, Kim K H, Lu R and Wu S-T 2008 *J. Phys. D: Appl. Phys.* **41** 055401
[20] Suwa S, Isozaki T, Inoue Y, Nakamura M, Miyakawa M and Urabe T 2010 *Soc. Inform. Disp. Tech. Dig.* **41** 595
[21] Wu S-T and Yang D-K 2001 *Reflective Liquid Crystal Displays* (New York: Wiley) p 149 chapter 7
[22] Jin M Y, Lee T H, Jang S J, Bae J H and Kim J H 2007 *Japan. J. Appl. Phys.* **46** 1585
[23] Vorflusev V and Kumar S 1999 *Science* **283** 1903